Impacts of the fall 2007 California wildfires on surface ozone: Integrating local observations with global model simulations

G. G. Pfister,[1] C. Wiedinmyer,[1] and L. K. Emmons[1]

Received 20 May 2008; revised 4 September 2008; accepted 9 September 2008; published 9 October 2008.

[1] This study quantifies the impact of the fires in California in fall 2007 on regional air quality and especially on surface ozone by analyzing surface observations of ozone concentrations together with global chemistry transport model simulations. The latter include a synthetic tracer providing information about the amount of ozone produced from the fires. It is shown that the global model is well suited for simulating the overall fire impact and a valuable tool for extracting information about the fire influence from the observations. A clear increase in observed ozone is found when the model predicts a strong impact of pollution from the fires, where measured afternoon 8-hour concentrations increased, on average, by about 10 ppb. The findings demonstrate that intense wildfire periods can significantly increase the frequency of ozone concentrations exceeding current U.S. health standards, and might cause violations also during photochemically less active seasons. The study also demonstrates the far-reaching impact of ozone production from the fires. **Citation:** Pfister, G. G., C. Wiedinmyer, and L. K. Emmons (2008), Impacts of the fall 2007 California wildfires on surface ozone: Integrating local observations with global model simulations, *Geophys. Res. Lett.*, *35*, L19814, doi:10.1029/2008GL034747.

1. Introduction

[2] Wildfires are a significant direct source of atmospheric pollutants such as carbon monoxide (CO), nitrogen oxides (NO_x), volatile organic compounds (VOCs) and particulate matter. The gaseous pollutants are precursors for ozone (O_3) production and as a result, wildfires have been proposed to lead to substantial increases in tropospheric O_3 concentrations [*Wotawa and Trainer*, 2000; *Cheng et al.*, 1998; *Crutzen and Andreae*, 1990]. Since O_3 is toxic in nature, elevated concentrations can have negative impacts on human health and plants. In 1997, the U.S. Environmental Protection Agency (EPA) set the 8-hour standard at 0.08 ppm, and in a recent update, which became effective in May 2008, lowered the standard to 0.075 ppm. In order to keep to these limits and help making decisions to reduce O_3 levels in areas where standards are exceeded, it is crucial to understand the individual contributions to the ozone budget.

[3] The major factors contributing to elevated pollution levels in the contiguous US include industry and transportation, but wildfires can also have a significant impact on air quality [*Bravo et al.*, 2002]. Nationwide, California is one of the states with the highest wildfire activity. In 2007, about 13 million acres burned across the US with California accounting for ~10% of the acres burned nationally (http://www.nifc.gov/fire_info/ytd_state.htm). The fire season in California typically starts around mid-May and ends around October, when cooler weather and increased precipitation conditions prevail. In fall 2007, severe drought conditions and hot weather contributed to an extremely intense late fire season. Fires in October were the most destructive of the year and in addition to severe drought conditions and hot weather, the unusually strong Santa Ana winds in Southern California were a major contributor. Numerous fires were ignited by broken powerlines, and the strong winds further hindered the progress of fire fighters.

[4] The purpose of this study is to quantify the impact of the fall 2007 fires in California on surface O_3 levels. Photochemistry is less active later in the year and exceedances of ozone health standards are generally less frequent. However, extreme events like wildfires might still have significant impacts on air quality especially when they occur during periods conducive to ozone formation.

2. Simulations, Observations, and Model Evaluation

[5] The simulations in this study are performed with the global chemistry transport model Model for Ozone and Related Chemical Tracers, version 4 (MOZART-4). Modifications from Version 2 published by *Horowitz et al.* [2003] include, amongst others, a more complete description of anthropogenic hydrocarbon chemistry, the inclusion of tropospheric aerosols (extended from the work of *Tie et al.* [2001, 2005]), and on-line calculations of photolysis rates, dry deposition, water vapor, and biogenic emissions. For a detailed model description we refer to L. K. Emmons et al. (Impact of Mexico City emissions on regional air quality from MOZART-4 simulations, manuscript in preparation, 2008) and for model evaluation to *Pfister et al.* [2005, 2006, 2008].

[6] The simulations were run at T85 (1.4° x 1.4°) spatial resolution using meteorological fields from NCEP-GFS (National Center for Environmental Prediction, Global Forecasting System). The vertical resolution of the model consists of 42 hybrid levels from the surface up to 2 hPa (~45 km). Of those, about 7 are within the lowest kilometer.

[7] Daily emissions of trace gases and particulate matter from the California fires were estimated using the framework described in detail by *Wiedinmyer et al.* [2006]. Using the MODIS thermal anomalies to determine fire location and timing, the emissions of CO_2, CO, NO_x, SO_2, and NH_3 were derived. Emissions of VOCs for the MOZART

[1]Atmospheric Chemistry Division, National Center for Atmospheric Research, Boulder, Colorado, USA.

0094-8276/08/2008GL034747$05.00

Table 1. Mean, Standard Deviation, Median, and Mean Difference *d* for Observed and Modeled 8-Hour Concentrations of O_3 and NO_2 for Individual Types of Monitoring Sites[a]

	Rural			Urban			Suburban		
	Obs	Model	d	Obs	Model	d	Obs	Model	d
				O_3					
all	44 ± 13 (42)	52 ± 13 (50)	8 ± 12	38 ± 12 (36)	53 ± 16 (50)	15 ± 13	41 ± 13 (39)	54 ± 17 (50)	13 ± 14
$O_3^{FIRE} \leq 0.5$ ppb	41 ± 11 (40)	49 ± 12 (48)	8 ± 10	36 ± 10 (35)	50 ± 15 (47)	15 ± 12	38 ± 12 (38)	51 ± 16 (48)	13 ± 13
$O_3^{FIRE} \geq 5$ ppb	51 ± 14 (49)	60 ± 12 (61)	9 ± 13	42 ± 15 (41)	61 ± 15 (62)	15 ± 17	46 ± 17 (45)	62 ± 16 (63)	16 ± 17
				NO_2					
All	7 ± 4 (6)	4 ± 3 (3)	−3 ± 5	13 ± 10 (10)	5 ± 4 (4)	−8 ± 8	14 ± 10 (11)	5 ± 4 (4)	−9 ± 8
$O_3^{FIRE} \leq 0.5$ ppb	7 ± 4 (6)	4 ± 4 (4)	−2 ± 5	13 ± 9 (11)	5 ± 4 (4)	−8 ± 8	14 ± 10 (12)	5 ± 4 (4)	−9 ± 8
$O_3^{FIRE} \geq 5$ ppb	6 ± 4 (5)	5 ± 2 (4)	−2 ± 4	17 ± 15 (10)	6 ± 4 (5)	−11 ± 13	18 ± 16 (11)	6 ± 5 (5)	−11 ± 13

[a]Observed and model median appears in parentheses. O_3 and NO_2 concentrations are in ppb. Results are given for all data and for two subsets of 8-hour O_3^{FIRE} concentrations. Values restricted to averages over 10–18 LT, 11–19T, and 12–20 LT for 1 Sep–30 Nov.

chemical mechanism (Emmons et al., manuscript in preparation, 2008; http://gctm.acd.ucar.edu/mozart) were determined from emitted CO_2 and the type of land cover burned in each fire pixel using emission factors from *Andreae and Merlet* [2001]. A time series of the total fire emissions over California is shown in the auxiliary material.[1] There were two main peaks in fire intensity, one in early September (estimated 5 GgN of emitted NO_x) and the other towards the end of October (estimated 7 GgN of emitted NO_x). In comparison, anthropogenic NO_x emissions over California are 40 GgN/month and global biomass burning emissions for September through December amount to 1950 GgN. California fire emissions for CO for this time period are 366 GgC and for VOCs 65 GgC.

[8] Global emissions from biofuel and fossil fuel combustion, aircraft, lightning, ocean, soil and vegetation are included in the model, primarily from the European Union project POET (Precursors of Ozone and their Effects in the Troposphere) [*Olivier et al.*, 2003]. Asian anthropogenic emissions are from *Ohara et al.* [2007]. Biomass burning emissions for outside California are based on a climatology derived from emission inventories available for previous years [*van der Werf et al.*, 2006]. While all emission inventories are subject to large uncertainties, often more than a factor of 2, [e.g., *van der Werf et al.*, 2006; *Wiedinmyer et al.*, 2006] and can be a major part of model uncertainties, their quantification is beyond the scope of this study.

[9] We incorporated two categories of chemical tracer schemes in the model. The first keeps track of the amount of CO emitted from the California fires (CO^{FIRE}), the other follows the O_3 production from NO emitted from the California fires (O_3^{FIRE}). The latter scheme tags the emitted NO and maintains the tag through all simulated odd nitrogen species (e.g. PAN, nitrates, HNO_3). We also tag the O_3 produced by the photolysis of tagged NO_2 (NO_2^{FIRE}). Except for some minor reactions, O_3 in the MOZART chemical mechanism is only produced through photolysis of NO_2. The scheme is described in greater detail by *Lamarque et al.* [2005], *Pfister et al.* [2006] and *Hess and Lamarque* [2007]. The model simulations are started 1 January 2007, and for September through November the model concentrations of CO, O_3, NO_2, and the respective fire tracers CO^{FIRE}, O_3^{FIRE} and NO_2^{FIRE} are output hourly.

[10] The observational data set includes measured surface O_3 concentrations for September–December 2007 provided by the EPA Aeromatic Information Retrieval System (AIRS) (EPA, U.S. Environmental Protection Agency air quality system data mart, 2008, available at http://www.epa.gov/ttn/airs/aqsdatamart). We use hourly observations from all sites in California and group them dependent on their location setting into rural sites (55), urban sites (38) and suburban sites (72). The model data are interpolated to the time step and location of the observations and both the modeled and observed 1-hour values are averaged into 8-hour concentrations, the standard used by the EPA for assessing ozone violations.

[11] Table 1 lists the mean and median observed and modeled 8-hour concentrations and the mean difference between the model and the observations for the three different site categories. We calculate statistics for the full data set, and also use O_3^{FIRE} to separately derive results for high ($O_3^{FIRE} \geq 5$ ppb) and low fire ($O_3^{FIRE} \leq 0.5$ ppb) impacted subsets. In support of the interpretation, we include a comparison of modeled and observed NO_2 concentrations for monitoring sites where NO_2 measurements are available (30 rural, 21 urban, 46 suburban).

[12] The model matches the observed 8-hour O_3 values generally to within 15 ppb, with correlation coefficients in the range 0.5–0.6. Both observations and model simulations show largest O_3 concentrations for the high fire impacted subset. As a result, the absolute difference between modeled and observed concentrations is higher for this data subset; however, the relative difference does not depend on the estimated degree of fire impact. Yet, the comparison does depend on the monitoring site category (urban, suburban, or rural). The observations show a clear difference between the individual site categories with lowest O_3 and highest NO_2 concentrations at urban sites and highest O_3 and lowest NO_2 concentrations at rural locations. The model in contrast simulates little variability between the mean concentrations for the different site categories. The modeled mean concentrations agree more closely with observations at the rural sites, while they overestimate O_3 and underestimate NO_2 values to a greater extent at urban and suburban sites. This result, however, is not surprising as the model covers California in 35 grid cells. Thus, the model is not able to resolve localized emission sources which are more likely to influence measurements taken in or near urban centers, but is better suited to represent conditions farther downwind from

[1]Auxiliary materials are available in the HTML. doi:10.1029/2008GL034747.

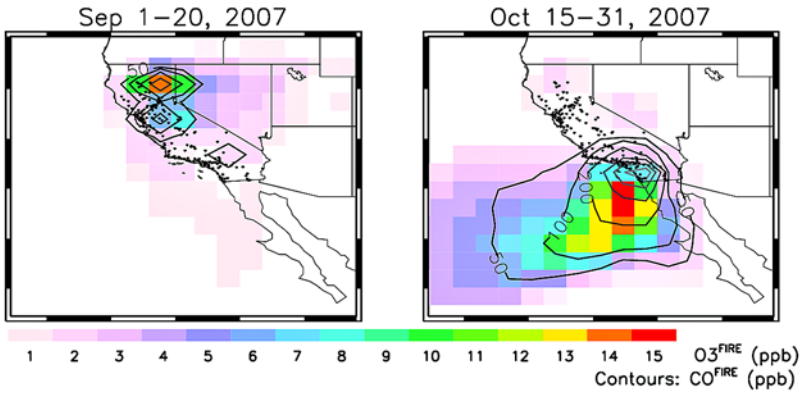

Figure 1. Mean modeled surface mixing ratios (ppb) for O_3^{FIRE} (filled contours) and CO^{FIRE} (contour lines) for (left) September 1–20 and (right) October 15–31. Dots indicate the locations of EPA monitoring sites.

source regions as is more characteristic of the rural monitoring sites.

3. Results and Discussion

[13] During the study period there were two main peaks in fire intensity. Fires during September took place mostly in the northern part of California, while fires in October were concentrated in the southern part of the state. Figure 1 shows the average concentrations of the model fire tracers O_3^{FIRE} and CO^{FIRE} for the two different time periods. The locations of the EPA monitoring sites are indicated in the plots.

[14] Our model tracers are restricted to tagging sources from within California, but it can be clearly seen that the impact of the fires reaches well beyond the state borders. During September, the California fires show a clear impact over large parts of Nevada, adding as much as 5 ppb to the modeled O_3 levels averaged over the fire period. In the October period, most of the fire pollutants were transported out over the ocean by the Santa Ana winds, which mitigated the impact on continental air quality.

[15] An interesting feature seen in Figure 1 is that the region of maximum impact of fire emitted CO does not necessarily co-locate with the maximum in O_3 produced from fire precursors. CO is directly emitted and the maximum impact occurs right over the source region. O_3, however, is chemically produced from fire-emitted precursors and the region of maximum impact is shifted downwind of the source region with the distance dependent on transport times and chemical regime. For October we actually find the region of maximum O_3^{FIRE} concentrations off the coast. Many modeling studies use CO tracers or passive tracers for determining the impacts of selected sources on trace gas budgets, but these results indicate that such a method can have significant shortcomings when looking at photochemically active species and especially when examining smaller spatial scales.

[16] From Figure 1 we find that the average model-estimated amount of O_3 produced from the fires can reach up to ~15 ppb when averaged over the fire period. To obtain an independent estimate, we analyze observations at the EPA monitoring sites along with information about the modeled fire impact. We group the entire data set of modeled and observed 8-hour values into two categories based on the timing of the fires: for one we select all data for 1–30 September, for the other all data for 8 October–8 November. Both time periods are chosen to include the time of most intense burning as well as about 2 weeks afterwards, or as in the case of October, a week before and a week after the fires. The separation of these shorter time periods helps to reduce the impacts of seasonal changes in photochemistry. We then calculate statistics of the observed and modeled 8-hour ozone concentrations binned by values of O_3^{FIRE} concentration, and do this for six subsets of data grouped by the two time periods stated above and by site category. The results are included in Figure 2 showing for both observations and model the absolute deviation from their respective mean concentration. Mean concentrations are calculated separately for each subset. We only include 8-hour concentrations centered in the local afternoon (10–18 LT, 11–19 LT, 12–20 LT) to preclude the results being impacted too strongly by the diurnal cycle in O_3 concentrations.

[17] Both model and observations show an overall increase in O_3 concentrations with increasing estimated fire impact. Best agreement is seen for rural sites, while the increase at urban and suburban sites is subject to higher variability and larger discrepancies between modeled and observed enhancements. This is due to the fact that the global model is less suited to simulating the urban environment (Section 2, Table 1) and for this reason we focus our quantitative analysis predominantly on rural monitoring sites. We find that the mean observed (modeled) enhancement in 8-hour O_3 concentrations for $O_3^{FIRE} > 10$ ppb is 9 ± 14 ppb (8 ± 11 ppb) for September and 8 ± 12 ppb (8 ± 11 ppb) for October. The percentages of data points in these categories are 10% and 7%, respectively. For data corresponding to $O_3^{FIRE} > 20$ ppb, the observed (modeled) enhancements increase to 12 ± 14 ppb (10 ± 10 ppb) for September and 10 ± 13 ppb (12 ± 9 ppb) for October. 5% and 3% of the data fall into these categories, respectively.

[18] Varying conditions of photochemical productivity (e.g. changes in temperature or cloudiness) can have an impact on the above statistics and to test this we repeated the calculations for different limitations of the data subsets by varying the length of the time periods chosen or selecting stations for different latitudinal zones. In either case, the general conclusions remain the same giving confidence that

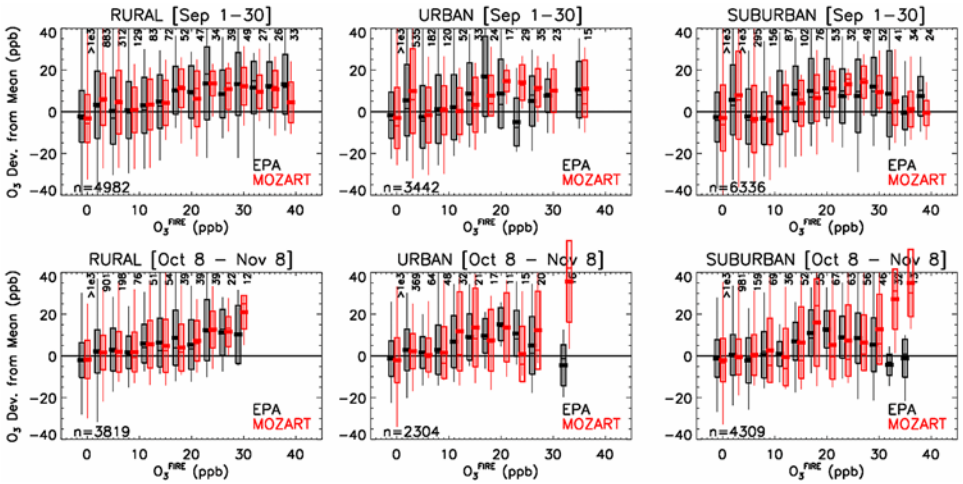

Figure 2. Observed and modeled 8-hour O_3 concentrations for 10–18 LT, 11–19LT and 12–20 LT binned by the fire tracer O_3^{FIRE}. Shown is the deviation from the mean concentrations (ppb); results are shown for rural, urban and suburban sites, and for the two main fire periods (Sep 1–30 and Oct 8–Nov 8). The number of data points in each category is indicated in the upper part of each plot, the total number of data points in the lower left corner. See text for more details.

changes in photochemical conditions have a small impact on the results. We also examined using CO^{FIRE} instead of O_3^{FIRE} as a tracer (not shown here). In that case we also detect a positive trend, but we identify fewer statistically significant results and see a larger variability because of the lack of co-location of peaks in CO^{FIRE} and peaks in O_3^{FIRE}.

[19] At urban and suburban sites, the model shows a tendency to overestimate the magnitude of fire impact on O_3 concentrations, which is in line with the model underestimate of NO_2 at urban and suburban sites (Section 2). The model dilutes the high pollution concentrations in urban environments, mainly due to the coarse model resolution. Adding additional NO_x in a less polluted environment causes a larger ozone increase compared to a NO_x and VOC richer environment. In support of this statement, we show in Figure 3 the modeled relationship between NO_2^{FIRE} and O_3^{FIRE} concentrations for three different NO_x regimes. The latter is estimated by subtracting NO_2^{FIRE} from total NO_2 concentrations. For the same amount of NO_2^{FIRE}, the NO_x poor environment generally gives a larger increase in O_3^{FIRE} compared to a NO_x rich environment. While these statistics point towards a stronger fire impact at rural versus urban sites, we cannot provide clear proof with the available data set.

[20] Finally, we also use the data sets to investigate the frequency of ozone exceedances (8-hour average O_3 > 0.08 ppm). For this purpose we calculate the maximum observed 8-hour O_3 value and the corresponding O_3^{FIRE} tracer value for each day at each rural monitoring site. There are 81 occurrences of O_3^{FIRE} > 15 ppb, and in 17% of these the observed O_3 concentrations exceeded the limit of 0.08 ppm. For O_3^{FIRE} > 10 ppb (n = 116) the frequency of exceedances is 12%, and for O_3^{FIRE} > 1 ppb (n = 434) it is 11%. In comparison, when O_3^{FIRE} < 1 ppb (n = 367), exceedances occur only 5% of the time.

[21] In total there are 66 exceedances for September through October. Only three of them occur in October, the first at the beginning of the month with a small estimated fire contribution (O_3^{FIRE}~1ppb), while the two later in the month occurred during the time of the fires with O_3^{FIRE} > 15 ppb. There might have been more violations if the winds hat not moved a major part of the pollution offshore (Figure 1).

[22] Revising the calculations for the new public health standard of 0.075 ppm, the number of exceedances nearly doubles and measured concentrations exceed the 0.075 ppm level 32% of the time when O_3^{FIRE} > 15 ppb, 17% of the time when O_3^{FIRE} > 1 ppb, and 9% of the time when O_3^{FIRE} < 1 ppb.

4. Conclusions

[23] We used a combination of surface observations of ozone and global model simulations to quantify the impacts of the California fires in autumn 2007 on surface ozone. For this purpose an O_3 fire tracer is incorporated into the model keeping track of the amount of O_3

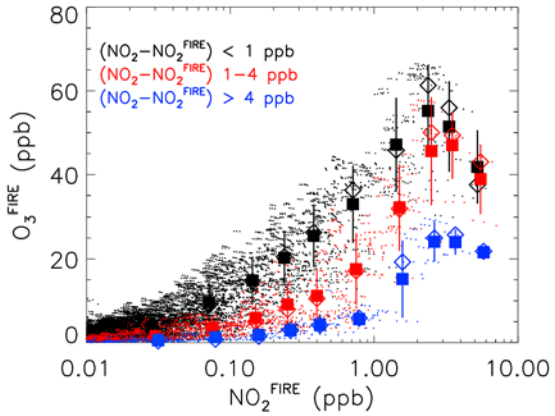

Figure 3. Relationship between surface concentrations of the model fire tracers NO_2^{FIRE} and O_3^{FIRE}. Mean (■), median (◇) and standard deviation of NO_2^{FIRE} bins are plotted over individual data points. Data are grouped into different NO_x regimes estimated by subtracting NO_2^{FIRE} from total NO_2 concentrations. Data set is limited to the month of September and to local afternoon values to limit the impact of temporal changes in photochemistry.

produced from fire-emitted NO and providing essential information for extracting quantitative information from the observations.

[24] Even though the spatial resolution of a global model limits resolving the differences between urban and rural environments, the combination of the modeled fire impact with a set of surface observations has been shown to be valuable in estimating the impact of the fires on surface O_3. We find a clear increase in observed surface O_3 when the model predicts the observations to be impacted by the fires with, on average, an enhancement of about 10 ppb in afternoon 8-hour concentrations for cases of high fire impact. Data and model analysis indicate that the less polluted areas (i.e. low NO_x environment) generally experience a stronger impact, but further studies are needed to confirm this.

[25] A major part of incidences when observed 8-hour concentrations exceeded the public health standards are associated with clearly elevated concentrations of the model O_3 fire tracer: exceedances occurred in 17% of the cases when the fire tracer was larger than 15 ppb and in 11% when the fire tracer was greater than 1 ppb. In comparison, for fire tracer concentrations less than 1 ppb, the frequency of occurrence of exceedances is 5%. Our findings demonstrate a clear impact of wildfires on surface O_3 nearby and potentially far downwind from the fire location, and show that intense wildfire periods frequently can cause O_3 levels to exceed current health standards.

[26] **Acknowledgments.** The authors acknowledge Jean-François Lamarque and Mary Barth for valuable input to the manuscript. The work was supported by NASA grants NNG06GB27G and NNX07AL57G. NCAR is operated by the University Corporation of Atmospheric Research under sponsorship of the National Science Foundation.

References

Andreae, M. O., and P. Merlet (2001), Emission of trace gases and aerosols from biomass burning, *Global Biogeochem. Cycles*, *15*, 955–966.

Bravo, A. H., E. R. Sosa, A. P. Sanchez, P. M. Jaimes, and R. M. I. Saavedra (2002), Impact of wildfires on air quality of Mexico City, 1992–1999, *Environ. Pollut.*, *117*, 243–253.

Cheng, L., K. M. McDonald, R. P. Angle, and H. S. Sandhu (1998), Forest fire enhanced photochemical air pollution: A case study, *Atmos. Environ.*, *32*, 673–681.

Crutzen, J. P., and M. O. Andreae (1990), Biomass burning in the tropics: Impact on atmospheric chemistry and biogeochemical cycles, *Science*, *250*, 1669–1678.

Hess, P. G., and J.-F. Lamarque (2007), Ozone source attribution and its modulation by the Arctic oscillation during the spring months, *J. Geophys. Res.*, *112*, D11303, doi:10.1029/2006JD007557.

Horowitz, L. W., et al. (2003), A global simulation of tropospheric ozone and related tracers: Description and evaluation of MOZART, version 2, *J. Geophys. Res.*, *108*(D24), 4784, doi:10.1029/2002JD002853.

Lamarque, J.-F., P. Hess, L. Emmons, L. Buja, W. Washington, and C. Granier (2005), Tropospheric ozone evolution between 1890 and 1990, *J. Geophys. Res.*, *110*, D08304, doi:10.1029/2004JD005537.

Ohara, T., H. Akimoto, J. Kurokawa, N. Horii, K. Yamaji, X. Yan, and T. Hayasaka (2007), An Asian emission inventory of anthropogenic emission sources for the period 1980–2020, *Atmos. Chem. Phys.*, *7*, 4419–4444.

Olivier, J. et al. (2003), Present and future surface emissions of atmospheric compounds, EU project EVK2-1999-00011, *POET Rep. 2*, Inst. Pierre Simon Laplace, Palaiseau, France. (Available at http://www.aero.jussieu.fr/projet/ACCENT/POET.php)

Pfister, G., P. G. Hess, L. K. Emmons, J.-F. Lamarque, C. Wiedinmyer, D. P. Edwards, G. Pétron, J. C. Gille, and G. W. Sachse (2005), Quantifying CO emissions from the 2004 Alaskan wildfires using MOPITT CO data, *Geophys. Res. Lett.*, *32*, L11809, doi:10.1029/2005GL022995.

Pfister, G. G., et al. (2006), Ozone production from the 2004 North American boreal fires, *J. Geophys. Res.*, *111*, D24S07, doi:10.1029/2006JD007695.

Pfister, G. G., P. G. Hess, L. K. Emmons, P. J. Rasch, and F. M. Vitt (2008), Impact of the summer 2004 Alaska fires on top of the atmosphere clear-sky radiation fluxes, *J. Geophys. Res.*, *113*, D02204, doi:10.1029/2007JD008797.

Tie, X., G. Brasseur, L. Emmons, L. Horowitz, and D. Kinnison (2001), Effects of aerosols on tropospheric oxidants: A global model study, *J. Geophys. Res.*, *106*, 22,931–22,964.

Tie, X., S. Madronich, S. Walters, D. P. Edwards, P. Ginoux, N. Mahowald, R. Zhang, C. Lou, and G. Brasseur (2005), Assessment of the global impact of aerosols on tropospheric oxidants, *J. Geophys. Res.*, *110*, D03204, doi:10.1029/2004JD005359.

van der Werf, G. R., et al. (2006), Interannual variability of global biomass burning emissions from 1997 to 2004, *Atmos. Chem. Phys.*, *6*, 3423–3441.

Wiedinmyer, C., B. Quayle, C. Geron, A. Belote, D. McKenzie, X. Zhang, S. O'Neill, and K. K. Wynne (2006), Estimating emissions from fires in North America for air quality modeling, *Atmos. Environ.*, *40*, 3419–3432.

Wotawa, G., and M. Trainer (2000), The influence of Canadian forest fires on pollutant concentrations in the United States, *Science*, *288*, 324–328, doi:10.1126/science.288.5464.324.

L. K. Emmons, G. G. Pfister, and C. Wiedinmyer, Atmospheric Chemistry Division, National Center for Atmospheric Research, P.O. Box 3000, 1850 Table Mesa Drive, Boulder, CO 80307, USA. (pfister@ucar.edu)